

Nonlinear dynamic soil-structure coupling analysis in steel structures on a wide foundation under near- and far-fault earthquakes using viscous energy absorbing systems

Ali Sanaeirad*, Reza Mohammadi

Department of Civil Engineering, Faculty of Engineering, Arak University, Arak, Iran

(Communicated by Asadollah Aghajani)

Abstract

Analysis of dynamic soil-structure interaction in steel structures with a wide foundation, as well as the use of appropriate energy-absorbing systems in structures whose members do not perform properly, is of great importance. This is because by absorbing seismic energy, these systems ensure that the structural members remain within the elastic range during an earthquake. Viscous dampers are among the energy dissipation devices that have been widely considered in modern seismic design methods. Given that loading codes change every few years, existing structures often no longer meet the provisions of new regulations and require retrofitting. This makes the idea of using a type of damper in these structures very significant. When performing correctly, these earthquake energy absorbers delay the structure's reaching the limit state during severe earthquakes, which is highly effective in improving structural performance. In this study, to investigate the role of interaction, the response of structures was compared from the perspective of inter-story drift and the behavior of structural members, both with and without considering dynamic soil-structure interaction and under near- and far-fault earthquakes. For this purpose, three two-dimensional steel moment frames with 10, 5, and 15 stories were used as low-rise, mid-rise, and high-rise structures, respectively. Then, the frames, which had been previously designed with viscous damper reinforcement and considering soil-structure interaction in loose soils, were analyzed. For the nonlinear dynamic analysis, seven accelerograms were used, and the results were compared. Based on the findings, it is observed that the reduction in floor response when using viscous dampers is not necessarily guaranteed; it can also increase depending on the earthquake record and the characteristics of the structure. The response of structures equipped with viscous dampers is close to that of structures without dampers, and in some cases, they are schematically almost identical. The results of the study indicate a significant increase in structural response in the presence of interaction and successive earthquakes, especially in low-rise buildings compared to high-rise buildings. These findings can be effective in improving seismic design criteria and evaluating the performance of structures against sequential earthquake events.

Keywords: dynamic soil-structure interaction, extensive foundation, near-fault double-quake earthquakes, nonlinear analysis, steel structure, seismic effects

2020 MSC: Primary 74L05; Secondary 74H15, 74H50, 74S05, 74K10, 86A15

*Corresponding author

Email addresses: a-sanaeirad@araku.ac.ir (Ali Sanaeirad), rezaitally@yahoo.com (Reza Mohammadi)

1 Introduction

In recent decades, the recurrence of devastating earthquakes in different parts of the world, especially in seismic areas such as Iran, has led to increasing attention to the detailed analysis of the behavior of structures against earthquakes. Iran, being located on an earthquake belt, has always been exposed to high-magnitude earthquakes that have led to extensive financial and human losses [3]. Among them, one of the phenomena that has been less comprehensively studied in seismic design is the effect of a sequence of successive earthquakes and the interaction between the structure and the soil beneath it [4]. In real conditions, structures may be damaged after an earthquake but still remain usable; in this case, subsequent earthquakes can cause further damage and even collapse without any reinforcement [5]. This issue becomes doubly important when considering the effects of soil-structure interaction, because dynamic interaction leads to changes in the stiffness, damping, and behavior of the entire structural system, and greatly alters the seismic response [7]. Conventional seismic analyses often model the soil under the structure as rigid; whereas in reality, the soil is flexible and significantly affects the dynamic response of the structure [1, 3]. This is especially important in construction sites with soft soil or great depth, because the intensity of the interaction effect also increases with increasing soil depth [1].

With the advancement of technology and the development of high-rise constructions, it seems necessary to carefully examine the effect of dynamic soil-structure interaction in combination with the seismic sequence phenomenon. Inertial and kinematic interactions cause changes in the natural period, stiffness, and vibration modes of structures, which have a significant impact on seismic design [2, 3]. A detailed understanding of the behavior of structures under earthquakes, without considering the dynamic interaction of soil and structure, leads to incorrect simplifications in seismic design. Soil-structure interaction is one of the fundamental topics in earthquake engineering, which is analyzed at two static and dynamic levels [15]. In the static case, it is assumed that the structure consists of three components: soil, foundation, and superstructure, and the distribution of stresses and deformations in these components is interdependent. In these analyses, the behavior of the soil is usually modeled with the Winkler model or elastic halfspace, and parameters such as the relative stiffness of the system, the bed modulus, and the stress distribution under the foundation are carefully examined [6].

In the dynamic case, the interaction is more complex, as the vibration of the structure causes changes in the dynamic response of the entire soil-structure system. These changes include an increase in the natural period of the structure, a decrease in the effective stiffness, and the transfer of additional damping from the soil environment to the structure [1, 3]. Previous studies have shown that structures located on soft soils are subject to a significant increase in displacement, floor drift, and a decrease in stability resistance, especially under conditions of successive excitations [8, 9]. Numerous studies have been conducted using numerical methods such as finite element, boundary element, and coupled analysis between structural and geotechnical software. For example, in dynamic modeling, the use of a hybrid analysis between SAP2000 for frame modeling and FLAC3D for soil half-space modeling has enabled a detailed investigation of the two-way interaction [1, 4]. The results of these modelings show that by considering the interaction, the response of the structure to severe earthquakes, especially in high-rise structures, increases significantly [1, 3, 5].

On the other hand, in the field of building structures, extensive research has been conducted on the vulnerability of unreinforced brick walls to lateral and cyclic loads. These walls have poor performance against earthquakes due to their brittle mechanical properties, heterogeneous behavior, and low tensile strength [2, 15]. In experiments conducted by Aramesh et al. [2], the behavior of brick walls under uniform and cyclic loads was investigated and the results showed that axial stresses, geometric aspect ratio, and type of crack (shear or bending) have a significant effect on ductility and ultimate strength.

The investigation of hysteresis curves in these walls has shown that although the masonry materials have a good energy dissipation capacity after initial cracking, their ultimate behavior is nonlinear and prone to sudden failure [2, 8, 15]. This is especially exacerbated in the presence of openings, flexible floors, and inefficient connections between walls [9]. In the past decades, many laboratory studies based on shaking tables have been conducted to evaluate the dynamic response of unreinforced or semi-reinforced masonry structures under real earthquake conditions. For example, Guo et al. [8], He et al. [9], and Hu et al. and Ji et al. [10, 11] are among the researchers who have investigated the effects of reinforcement, type of floor system, and wall connection on the response of the structure to dynamic loading. Their results indicate that proper connection between the floor and the wall significantly increases the lateral resistance of the building [9, 10, 12]. Also, in joint international laboratory projects, including the joint Italy-USA project, results have shown that unreinforced walls can regain some of their load-bearing capacity if properly repaired and strengthened [13, 16, 17]. These findings reinforce the need to consider the effects of structure-soil interaction in addition to the effects of brittle materials. Supplementary numerical studies on soil-structure systems have investigated the effects of soil type (type I and III), model boundary conditions, soil depth, and seismic load combinations. According to the results obtained, in soft soils (type III), the interaction is more pronounced and the

increase in floor drift, especially in tall structures, reaches more than twice the case without interaction [1, 4, 18]. Also, by successively applying two real earthquakes such as Tabas and Kobe, it was observed that the cumulative effects of the seismic response are intensified, both in the soil environment and in the structure [4, 18].

A study was conducted on the effect of dynamic soil-structure interaction on the seismic behavior of tall structures. They investigated a soil-structure numerical model using Abaqus software to evaluate the effect of soil-structure interaction on tall steel structures with tubular structure system. The results showed that soil-structure interaction has a significant effect on the seismic behavior of tall structures with tubular core; Because it can increase the lateral displacement and drift of the stories and also reduce the shear of the stories [13].

They conducted a study on the effect of soil-structure interaction on the seismic behavior of frames with base seismic isolation under the influence of earthquakes in the near- and far-fault areas. They found that for frames with base seismic isolation, considering soil-structure interaction does not have a significant effect on the lateral displacement results of the stories of short- and medium-rise models; but in the high-rise frame with soft soil in the near-fault area, it is up to 80% higher. They also showed that considering the effect of soil-structure interaction for frames with fixed foundations, especially in higher stories, reduces the acceleration of the stories [16].

Kontoni and Farghaly [17] conducted a study on the effects of structure-soil-structure interaction on the seismic response of adjacent high-rise structures equipped with tuned mass dampers. They showed that the use of tuned mass dampers with optimal parameters in 20-story structures can reduce the response of the structures both in the fixed base case and by considering the structure-soil-structure interaction. However, considering the structure-soil-structure interaction causes changes in the responses of the structures equipped with the dampers; such that these changes are incremental in the structure with a higher (slimmer) aspect ratio. Also, in order to determine the characteristics of mass dampers in high-rise structures with close vibration periods, it is better to consider the effects of the structure-soil-structure interaction [17]. In summary of previous studies, it can be said that most of the existing research has either only investigated the interaction in a single earthquake or has only focused on the response of building materials. While the simultaneous effect of soil-structure dynamic interaction and the occurrence of successive earthquakes is a less studied topic and has a serious research gap. Generally, the philosophy of designing structures against earthquakes has been based on studies conducted in the fixed footing mode. Although this assumption is correct for structures located on rocky beds, it is far from reality for structures located on soft soil. Most of the studies conducted on the nonlinear behavior of structures have been in the fixed footing mode, and in the soil-structure interaction mode, except for a few studies on single-degree-of-freedom structures, not much research has been conducted. Since soil-structure interaction has a significant effect on the nonlinear response of single-degree-offreedom structures, it is expected to change the inelastic behavior of multi-degree-of-freedom structures as well. Experiences of the last decade have shown that the effects of soil-structure interaction in massive, heavy and rigid buildings built on weak and soft soils are significant in terms of their stability. The materials presented here demonstrate the importance of considering soil-structure interaction. Although extensive research has been conducted in the field of soilstructure interaction and viscous dampers separately, there has been no research on the behavior of steel structures using Pal dampers considering the interaction between structure and soil. In this study, we will try to investigate the deformations of the structure, the base shear forces, and the internal forces of the members using the effect of viscous dampers and soil interaction.

2 Materials and research methods

2.1 Methods used in the analysis

The present research is of an applied nature. Theoretical information and research background were collected by studying various sources and references, including books, articles, and websites.

For the modeling section, we used two-dimensional steel moment frame models of 5, 10, and 15 stories. These models were equipped with viscous dampers installed on figure-8 braces. The span length, floor height, and load-bearing width were set at five, three, and five meters, respectively, in accordance with the specifications of conventional buildings.

The software used for modeling and analysis was SAP2000. For loading and the initial design of structural members, we followed topics six and ten of the National Building Regulations. The dead and live loads for the frames, assuming residential use, were set at 500 kg/m^2 and 200 kg/m^2 , respectively. For seismic loading, the structures' location was considered an area with a very high seismic hazard and various soil types.

Finally, the structural responses, including displacements and foundation shear, were compared before and after improving a specific form of the wide foundation. This comparison was based on a nonlinear dynamic analysis, considering the effect of soil-structure interaction both with and without it.

2.2 Soil-structure interaction

During an earthquake, the response of a structure and the ground are mutually dependent. Loads transferred from the structure to the foundation affect both the concrete foundation and the surrounding soil, causing stresses and deformations. The presence of a structure can even change how the ground vibrates in its vicinity compared to a bare soil site. Conversely, deformations in the foundation and soil alter the dynamic response of the structure [19, 21].

Therefore, it can be concluded that the structure, foundation, and underlying soil collectively behave as a single system. Each component's characteristics affect the others, a phenomenon known as interaction. This concept led to a new field in seismic geotechnical science called soil-foundation-structure interaction, which seeks to simultaneously account for these factors in structural analysis and design [22, 23].

While the effect of soil on a structure's performance during an earthquake has recently garnered significant attention from researchers, studies have primarily focused on site effects, with less attention paid to the broader phenomenon of soil-structure interaction (SSI). A common method for evaluating a structure's response is to apply an earthquake record at its base, assuming a rigid foundation. While this assumption is valid for structures on rock, increasing soil flexibility leads to significant changes in structural behavior due to SSI.

Evaluating the dynamic response of a structure by considering SSI involves treating the structure as part of a larger soil-structure system. This has two major effects: first, it increases the system's degrees of freedom and changes its dynamic characteristics; second, it leads to the dissipation of a portion of the seismic energy into the soil. As a result, the soil-structure system will have a longer natural period compared to a model with a rigid base. Therefore, the assumption of a rigid connection to the ground is a simplifying one that is not always correct. Mylonakis and Gazetas [20] showed that including soil-foundation interaction leads to a more realistic structural behavior. In essence, the presence of soft soil under the structure reduces the overall system's stiffness, increases its natural period, and causes the structure to exhibit a more flexible behavior.

There are various mechanisms for soil-structure interaction, including kinematic interaction, inertial interaction, and a combination of both [24].

Kinematic interaction can be defined as follows: In free-field soil, an earthquake causes soil displacements in both horizontal and vertical directions. If a surface or embedded foundation is so stiff that it cannot conform to these free-field deformations, its motion will be affected by kinematic interaction, even if it has no mass. For instance, the flexural stiffness of a massless wide foundation (Figure 1) prevents it from following the horizontal variations of the vertical component of free-field soil motion. Similarly, the stiffness of a massless buried foundation (Figure 1) prevents it from following the vertical variations in horizontal free-field motion. The axial stiffness of a pile foundation (Figure 1) prevents the spread of discontinuous free-field soil motion. In each of these cases, the foundation's motion is influenced by kinematic interaction. However, kinematic interaction does not occur in all cases. For example, if the foundation is subjected to vertically propagating S-waves (which cause only horizontal particle motion), the soil displacement is not constrained, and kinematic interaction does not occur. Kinematic interaction happens when the stiffness of the system prevents the propagation of free ground motions.

The edited version improves the text's clarity and flow by correcting grammatical errors, adjusting phrasing for a more academic tone, and restructuring some sentences for better readability. For instance, I've clarified technical terms and ensured a more consistent tense throughout.

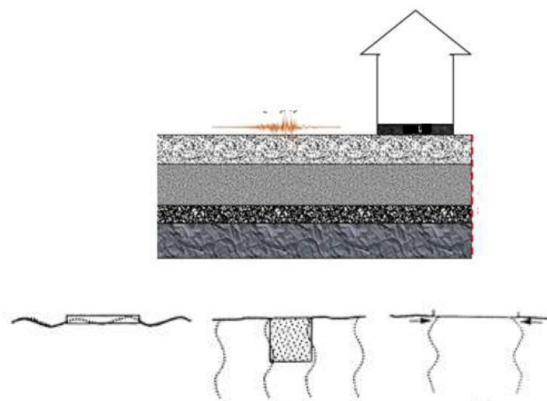


Figure 1: Structure, foundation and soil and types of foundation stiffness

The deformations resulting from the kinematic interaction can be determined by assuming that the foundation is rigid but not mass. The equations of motion for this case are:

$$[M]\{\ddot{u}_{KI}\} + [K^*]\{u_{KI}\} = -Mr\ddot{u}_g(t)$$

For inertial interaction, we have: Since the structure and foundation have mass, this mass causes their dynamic response. If the bed soil is ductile, the forces transferred from the foundation to it cause the foundation to move. The effects of soil ductility changes on the resulting response are due to the inertial interaction. The deformations resulting from the inertial interaction can be calculated from the equation of motion below.

$$[M_s]\{\ddot{u}_{II}\} + [K^*]\{u_{II}\} = -[M_z]\{\ddot{u}_{KI}(t) + \ddot{u}_b(t)\}$$

In the above relation, $[M_s]$ is the mass matrix of the structure, assuming that the soil is massless. It is worth noting that the right-hand side of the above equation indicates the inertial loading on the structure-foundation system. This inertial loading depends on the base motion and the input motion of the foundation, which reflects the effects of kinematic interaction. In inertial interaction analysis, the inertial loading is applied only to the structure, and the soil mass base is motionless (Figure 2).

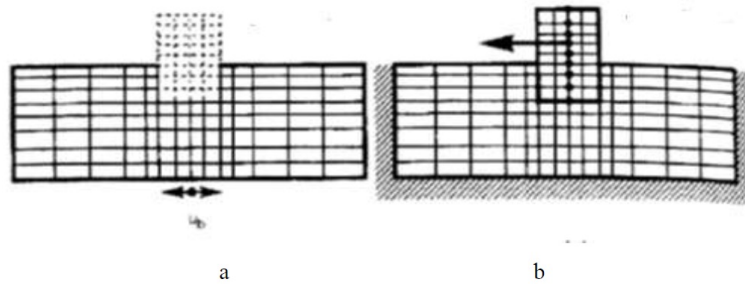


Figure 2: (a) Kinematic interaction analysis and (b) Inertial interaction analysis

Combining kinematic and inertial interaction, we have: Kinematic interaction analyses produce the massless foundation-structure system motion (relative to the support) resulting from the kinematic interaction. This motion is combined with the support motion to produce the kinetic motion of the entire system. When the inertial loading resulting from this kinetic motion is applied to the foundation-structure system resting on a massless soil bed,

$$[M]\{\ddot{u}_{KI}\} + [M_{Tot}]\{\ddot{u}_{II}\} + [K^*]\{\{u_{KI}\} + \{\ddot{u}_{KI}\}\} = -([M] + [M])\{\ddot{u}_b\} - [M]\{\ddot{u}_{KI}\}$$

2.3 Corrected and edited text

The methods for soil-structure interaction (SSI) analysis include two primary approaches: the direct method and the substructure method.

2.3.1 Direct method

In the direct method, the entire soil-foundation-structure system is modeled and analyzed in a single step. This approach doesn't require applying the principle of superposition, which allows for the use of nonlinear analyses. This study used the direct method because it focuses on the effects of nonlinear soil behavior and the consequences of support flexibility. One of this method's key features is its ability to account for geometric damping effects from the foundation's embedded depth, the structure's settlement in the soil, and the soil's stratification in both horizontal and vertical directions [25].

2.3.2 Substructure method

In the substructure method, the soil-foundation-structure assembly is modeled separately, with each component treated as a substructure. Each substructure is analyzed using its own appropriate method, and the results are then combined using the principle of superposition. This approach is considered a linear method and is generally used when assuming linear behavior for the soil and structure. To account for nonlinear behavior, an equivalent linear method can be used [27].

The most common method for solving the SSI problem is the substructure analysis method, where the entire soil-structure system is divided into three parts:

- Substructure I: The free-field soil of the construction site.
- Substructure II: The volume of soil removed during excavation.
- Substructure III: The superstructure and its foundation [26].

The corrections we've made focus on improving sentence structure, grammar, and technical vocabulary to make the text clearer and more professional. We've also used bolding to highlight key technical terms, which is common practice in academic writing.

2.4 Nonlinear dynamic analysis

Nonlinear dynamic analysis is performed using the Newmark beta integration method and the quasi-force method. The solution is performed step by step according to the following equation:

$$[M]\{\Delta\ddot{u}\} + [C]\{\Delta\dot{u}\} + [K_t]\{\Delta u\} = -[M](\{L_h\}\Delta\ddot{x}_{gh} + \{L_v\}\Delta\ddot{x}_{gv}) - \{\Delta P_v\} - \{\Delta P_{FR}\} - \{\Delta P_{HY}\} - \{\Delta P_{TW}\} + C_{corr}\{\Delta F_{err}\} \quad (2.1)$$

where $[M]$ is the concentrated mass matrix of the structure, $[C]$ is the damping matrix of the structure, $[K]$ is the tangent stiffness matrix, and are the velocity and acceleration of the structure, respectively.

The step-by-step solution is performed using the Newmark beta algorithm, which is based on the assumption that the acceleration changes during the motion are linear. Therefore:

$$\begin{aligned} \{\dot{u}\}_{t+\Delta t} &= \{\dot{u}\}_t + \Delta t[(1-\gamma)\{\ddot{u}\}_t + \gamma\{\ddot{u}\}_{t+\Delta t}] \\ \{u\}_{t+\Delta t} &= \{u\}_t + \Delta t\{\dot{u}\}_t + (\Delta t)^2[(0.5-\beta)\{\ddot{u}\}_t + \beta\{\ddot{u}\}_{t+\Delta t}] \end{aligned} \quad (2.2)$$

The IDARC software is conventionally set up to implement the Newmark constant acceleration unconditional stability method for dynamic analysis, in which

$$\begin{aligned} \beta &= 1.4 \\ \gamma &= 1.2 \end{aligned}$$

However, the above parameters may be changed to perform the analysis using the linear acceleration method as follows:

$$\begin{aligned} \beta &= 1.6 \\ \gamma &= 1.2 \end{aligned}$$

According to the above equations, the following relations are valid for the increase in acceleration rate:

$$\begin{aligned} \{\Delta\dot{u}\}_{t+\Delta t} &= \left(1 - \frac{\gamma}{2\beta}\right) \Delta t\{\ddot{u}\}_t - \frac{\gamma}{\beta}\{\dot{u}\}_t + \frac{\gamma}{\beta\Delta t}\{\Delta u\}_{t+\Delta t} \\ \{\Delta\ddot{u}\}_{t+\Delta t} &= \frac{1}{\gamma\Delta t}\{\Delta\dot{u}\}_{t+\Delta t} - \frac{1}{\gamma}\{\ddot{u}\}_t \end{aligned} \quad (2.3)$$

Substituting into the governing equation of motion, we obtain:

$$[K_D]\{\Delta u\}_{t+\Delta t} = \{\Delta F_D\} \quad (2.4)$$

$\{\Delta F_D\}$, $[K_D]$ are considered as equivalent dynamic stiffness and load vector. The solution is performed step by step assuming that the structural properties do not change during the time step. Since the stiffness of some elements may change during the time step, the new configuration may not satisfy the equilibrium equations, an error neutralization process is adopted by applying a one-step unbalanced force correction to minimize the error. At the end of the step, the difference between the force calculated using the hysteretic model ($\{R\}$) and the force calculated assuming no change in stiffness during the time step ($\{R'\}$) yields the unbalanced force (Figure 3).

This corrected force is applied at the next time step of the analysis. The unbalanced forces are calculated when the anchors, shears, and stiffness are corrected in the hysteretic model. Such a process was first performed in the DRAIN2D software [14] because the iteration cycle in nonlinear dynamic analysis is cumbersome and time-consuming,

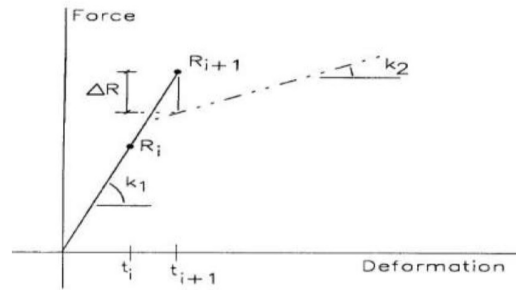


Figure 3: Unbalanced force correction

especially for large buildings. However, it should be noted that this technique is not physically accurate. Because the addition of unbalanced forces in the next step will affect the input loads. Such a method provides acceptable solutions when the unbalanced forces are small. To minimize the unbalanced forces, the analysis time step should be chosen small enough. Numerical instability in the program due to an inappropriate time step often leads to large unbalanced forces and creates a problem in the hysteretic behavior to track the actual responses of the members.

2.5 Unbalanced forces and analysis

The corrected force is applied at the next time step of the analysis. Unbalanced forces are calculated by correcting the anchors, shears, and stiffness in the hysteretic model. This process was first implemented in the DRAIN-2D software [14], as the iterative cycles in nonlinear dynamic analysis are cumbersome and time-consuming, especially for large buildings. However, it's important to note that this technique is not physically accurate because the addition of unbalanced forces in the next step will affect the input loads. This method provides acceptable solutions only when the unbalanced forces are small. To minimize these forces, the analysis time step must be chosen to be sufficiently small. Numerical instability caused by an inappropriate time step often leads to large unbalanced forces, which can hinder the hysteretic model's ability to accurately track the actual responses of the members.

2.6 Loading and structural modeling

To evaluate the performance of steel structures, considering soil interaction under near- and far-fault earthquake records, this study analyzed three steel structures:

1. A 5-story steel structure
2. A 10-story steel structure
3. A 15-story steel structure

These structures are designed with three 5-meter spans and a floor height of 3 meters. The material used is St37 steel with a modulus of elasticity of $2.1 \times 10^{10} \text{ kg/m}^2$ and a yield stress of $2.4 \times 10^7 \text{ kg/m}^2$. The modeling of these structures was performed using SAP2000 software.

1. Gravity Loading: The load-bearing surface of the beams is considered to be 4 meters in width. Assuming a dead load of 500 kg/m^2 and a live load of 200 kg/m^2 , the corresponding loads on the beams are:
 - Dead Load: 2000 kg/m
 - Live Load: 800 kg/m
2. Seismic Loading: The earthquake records used for this study are categorized into two groups:
 - (a) Near-fault earthquake records
 - (b) Far-fault earthquake records

Each set includes three earthquake records. Detailed specifications and characteristics of these records will be provided in a later section of this document.

Modeling Assumptions:

- Soil-Structure Interaction: To account for soil-structure interaction, linear springs are modeled at the supports (the base of the first-floor columns) in both the horizontal and vertical directions. The properties of these springs are determined by the soil characteristics and foundation dimensions. The theory behind this modeling approach and the specific calculations for this project will be discussed in the relevant section.

- Viscous Damper: The Link Support element in SAP2000 was used to model the viscous dampers. The necessary explanations regarding the location, stiffness, and damping values of the dampers will be provided in a dedicated section.

The text is now more concise and structured, making it easier for the reader to follow the methodology. It also uses more standard technical terminology.

Table 1: Structure specifications

Structure	Number of spans	Length of spans	Floor height	Column section	Beam section
5 floors	3	5	3	Box $30 \times 30 \times 1$	IP $25 \times 20 \times 1$
10 floors	3	5	3	Box $35 \times 35 \times 1$	IP $30 \times 25 \times 1$
15 floors	3	5	3	Box $40 \times 40 \times 1$	IP $40 \times 30 \times 1$

$$DL = 2000Kg/m$$

$$LL = 800Kg/m$$

3. Mass Source: In calculating the effective mass of the structure, the dead load plus 20% live load is considered. The materials used in the models are St37 with an elastic modulus of $10^{10} \times 2.1kg/m^2$. The yield stress is also considered to be $7^{10} \times 2.4kg/m^2$.

2.6.1 Modeling of structures

The modeling of structures has been done in Sap software and their schematic form is as follows:

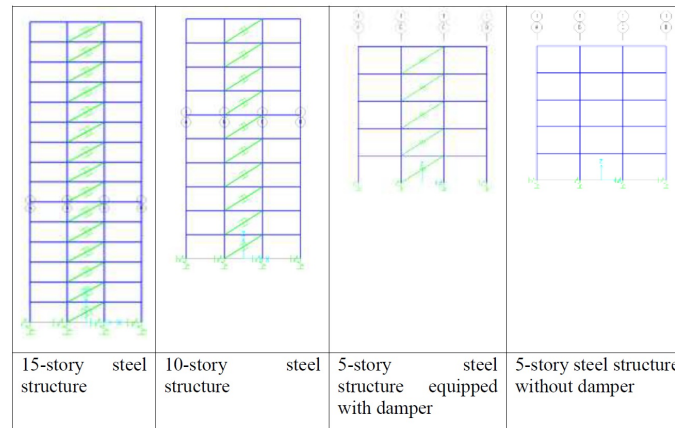


Figure 4: Modeling of structures

Earthquake records:

The earthquake records used in this study include three near-fault earthquake records and three along-fault earthquake records, a total of six earthquake records, as follows:

Table 2: Earthquake records used in this study

Duration	Earthquake characteristics	Earthquake name	Number
80 seconds	Fault radius	BORREGO	1
82 seconds	Fault radius	NCALIF	2
40 seconds	Fault radius	SCALIF	3
90 seconds	Near the fault	CHICHI	4
54 seconds	Near the fault	KOBE	5
28 seconds	Near the fault	LANDERS	6

The above earthquake records are scaled so that their elastic response spectrum in the main period of the structure is 0.3g. The damping factor applied to the structures in the time history analysis is 0.05. The time history analysis algorithm is the Newmark method with characteristic values $\beta = 0.25$ and $\gamma = 0.5$.

2.6.2 Problem solving method

The original text is a bit fragmented and contains some grammatical errors that are common in direct translations. Here is a revised and edited version that is more professional and academic in tone, ready for a technical paper or report. To model the soil beneath the foundation and account for its effects on the structure’s behavior, the substructure method is employed. In this method, the soil-structure system is divided into two parts: the first is the structure situated on the foundation, and the second is the soil, which shares a common boundary with the foundation. First, the soil’s force-displacement relationship is determined for the nodes at the common boundary. This relationship can be physically represented by a series of springs and dampers, whose coefficients depend on the excitation frequency. The structure is then placed on these springs. This approach breaks down a highly complex soil-structure system into two manageable parts, allowing for analysis to be performed at a lower computational cost. Although these methods generally involve approximations, the cone model is a newer and more user-friendly approach in this field. In the cone model, the soil beneath the foundation is assumed to be a diverging cone, and displacement is applied through the massless and rigid foundation. The principles used to derive the governing equations for these cones are based on the theory of beams, where a plane perpendicular to the neutral axis remains a plane after deformation. Using this principle, the spring and damper coefficients are calculated.

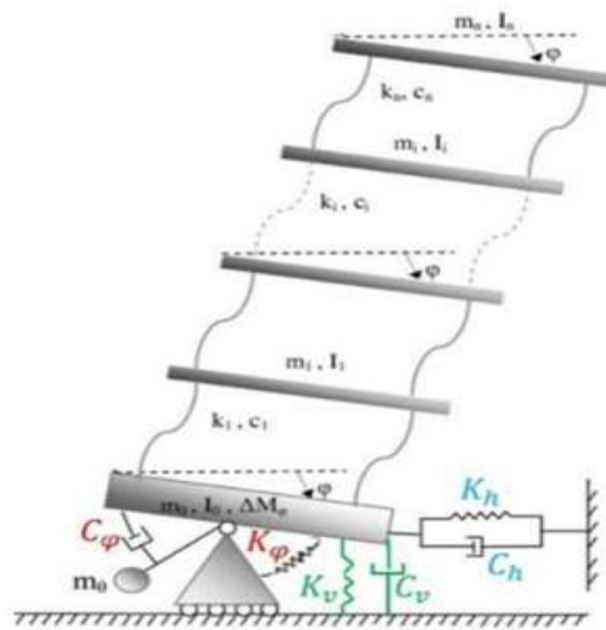


Figure 5: Schematic diagram of the substructure system

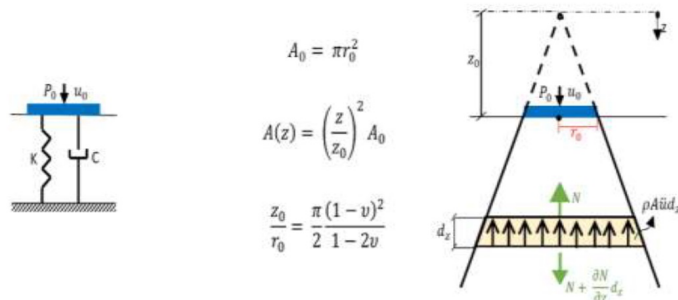


Figure 6: Cone models

Different cone models are defined based on the types of displacements created. Generally, cone models are divided into two categories: translational and rotational.

- A_0 : Foundation area

- r_0 : Equivalent radius of a circular foundation
- z_0 : Foundation height from the tip of the cone

The cone model provides more reliable approximation results than other methods. This is due to its conceptual clarity, simple physics, accurate mathematical response, practical application, and sufficient generality to handle layered soil for all degrees of freedom and all frequencies with adequate engineering accuracy. This edited version clarifies the relationship between the soil and the structure within the substructure method and provides a more professional description of the cone model.

2.6.3 Footing dimensions

The foundation dimensions of the modeled structures are considered as follows (Table 3):

Table 3: Footing dimensions of the modeled structures

Structure	5 floors	10 floors	15 floors
Foundation dimensions (meters)	1.5×1.5	2×2	2.5×2.5

2.6.4 Poisson's ratio of soil

Poisson's ratio for the soil under the foundation is considered to be 0.3.

Horizontal movement and Vertical movement

2.6.5 Shear wave velocity

The shear and vertical wave velocities are considered to be 80 and 150 m/s, respectively.

The soil specific gravity is considered to be 1900 kg/m^3 .

2.7 Soil modeling parameters

Since Poisson's ratio is equal to 0.3, according to the table "Cone Model and Damper-Mass Model", the aspect ratio z_0 to r_0 will be as follows (Table 4):

Table 4: Wave speed and equivalent radius

Equivalent radius	$\sqrt{\frac{A_0}{\pi}}$	
	Horizontal	Standing
Wave speed (C)	C=C _s =80m/s	C=C _p =150m/s

According to the above tables and relations, the vertical and horizontal stiffness at the foot of the columns will be as follows (Table 5):

Table 5: Vertical and horizontal stiffness at the foot of the columns

	5 floors	10 floors	15 floors
$A_0(m^2)$	2.25	4	6.25
$r_0(m)$	0.84	1.12	1.41
$z_{0v}(m)$	$1.93 \times 0.84 = 1.62$	$1.93 \times 1.12 = 2.16$	$1.93 \times 1.41 = 2.7$
$z_{0h}(m)$	$0.66 \times 0.84 = 0.55$	$0.66 \times 1.12 = 0.74$	$0.66 \times 1.41 = 0.93$
$k_v(N/m)$	$1900 \times 150^2 \times 2.25/1.62 = 59375000$	$1900 \times 150^2 \times 4/2.16 = 79166000$	$1900 \times 150^2 \times 6.25/2.7 = 98958000$
$k_h(N/m)$	$1900 \times 80^2 \times 2.25/1.62 = 16888000$	$1900 \times 80^2 \times 4/2.16 = 22518000$	$1900 \times 80^2 \times 6.25/2.7 = 28148000$

2.7.1 Viscous damper specifications

In order to build earthquake-resistant buildings, one of the economical methods is to use dampers or energy dissipation devices. Among them, viscous dampers are one of the types of energy dissipation devices that perform well in reducing the dynamic forces entering the structure and are considered among the most economical. This damper is actually a simple connection with a viscous screw that has long bean-shaped holes. The viscous damper is one of

the passive control systems that is placed at the bracing location. By absorbing part of the seismic energy entering the structure, this damper reduces the energy dissipation demand on the structural elements and minimizes structural damage. Conventional structures absorb energy through the yielding or rupture of building materials. For example, in steel beams and columns, seismic energy is absorbed by forming a plastic hinge, and in concrete structures by creating cracks. Viscous dampers offer a solution to yielding or failure. These dampers provide a force that always resists the movement of the structure.

Viscous dampers are one of the simplest types of energy dissipation devices in a structure. Such energy dissipation devices are designed using a viscous connection with bean-shaped holes as shown in the figure 7.



Figure 7: Viscous damper

If the force applied to the viscous connection is greater than the sliding load of the connection, the surfaces start to move suddenly. However, after movement, the amount of friction force changes compared to the start of movement, depending on the material of the contact surfaces, and these changes also differ depending on the range of displacement. Therefore, if a certain friction force can be created in a connection or a member so that the amount of this force can be controlled, the desired damper has been produced (Table 6). The characteristics of the viscous damper used in the structures are as follows:

Stiffness Ratio $10000kg/m$

Damping Ratio $10kg/s$

Table 6: Period of Structures

1.52 seconds	5 floors
2.2 seconds	10 floors
2.53 seconds	15 floors

The periodic period of the 10-story structure is greater than the Beqeh because its sections are defined in such a way that the beam section is weaker than the column section than other structures. The reason for this will be explained later.

3 Results

3.1 Results of the analysis of the 5-story structure (base shear and floor displacement)

According to the modeling, the results of the modeling of the 5-story structure during earthquakes far and near the fault were examined in two cases without viscous damper and with viscous damper. Their results are given in Table 7 and Figures 8 and 9.

According to the tables and diagrams of the results of the analysis of a 5-story structure without a viscous damper in the near and far areas of the fault, it can be inferred that the rate of increase in response has a uniform upward trend and all records of the schematic form are close to each other.

According to the tables and diagrams of the results of the analysis of a 5-story structure with a viscous damper in the near and far areas of the fault, it can be inferred that the responses of the structure equipped with a viscous damper are very close to each other and to some extent According to the tables and diagrams of the results of the

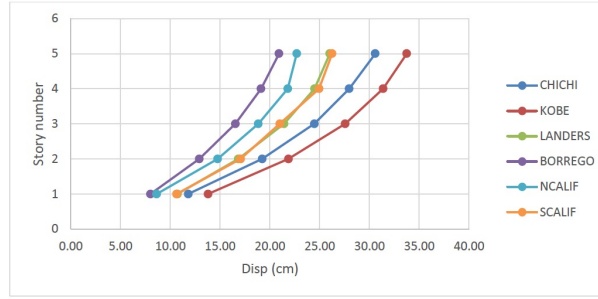


Figure 8: Diagram of the results of the analysis of a 5-story structure without a viscous damper in the near and far areas of the fault

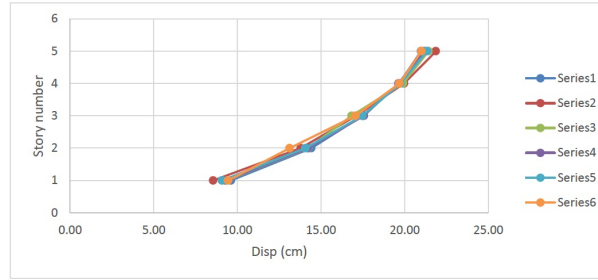


Figure 9: Diagram of the results of the analysis of a 5-story structure with a viscous damper in the near and far areas of the fault

analysis of a 5-story structure with a viscous damper in the near and far areas of the fault, it can be inferred that the responses of the structure equipped with a viscous damper are very close to each other and to some extent coincide. The percentage of reduction in the responses of the structure in the state equipped with a viscous damper compared to the state without a viscous damper is presented in the first table.

Table 7: Percentage reduction in structural responses in the case of equipped with viscous dampers compared to the case without viscous dampers

	BORREGO	Fault radius			Near the fault		
		NCALIF	SCALIF	CHICHI	KOBE	LANDERS	
Basic cutting		-29.77%	-8.86%	0.95%	15.91%	35.18%	18.13%
Lateral movement of floors	5th floor	-1.23%	6.00%	20.00%	31.43%	35.21%	17.65%
	4th floor	-2.70%	9.38%	21.05%	29.69%	36.36%	18.75%
	3th floor	-6.25%	7.23%	18.75%	28.57%	37.93%	21.43%
	2th floor	-10.00%	4.62%	23.08%	25.00%	36.96%	15.45%
	1th floor	-16.13%	-5.26%	11.11%	18.52%	37.93%	12.86%

According to the numbers in the table above, it can be said that the reduction in the lateral displacement of the floors and the base shear of the 5-story steel structure has decreased significantly under near-fault records. But this reduction is negative under the BORREGO earthquake record. That is, with the structure equipped with viscous dampers, the displacement and base shear have increased. But in the NCALIF and SCALIF earthquake records, we are mainly faced with a decrease in response.

3.2 Results of analysis of the 10-story structure (base shear and floor displacement)

According to the modeling, the results of modeling the 10-story structure during earthquakes far and near the fault in two cases without viscous dampers and with viscous dampers were examined. Their results are given in Figures 10 and 11.

According to the above diagram and tables, it can be seen that the lateral displacement of the floors is uniformly increasing.

It is clear from the above diagram that the responses of the 10-story steel structure equipped with viscous damper are also close to each other. And from the 6th floor onwards, a sudden increase in the response of the structure is observed (Table 8).

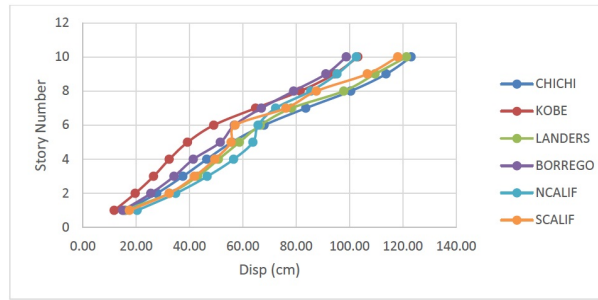


Figure 10: Displacement diagram of a 10-story steel structure without viscous damper

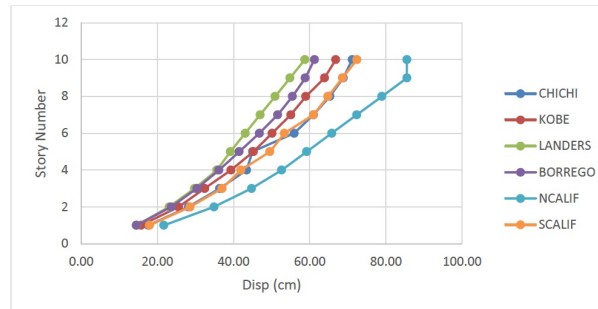


Figure 11: Displacement diagram of a 10-story steel structure equipped with viscous damper

Table 8: Percentage of reduction in structural responses in the case equipped with viscous damper to the case without viscous damper (near the fault)

	CHICHI	Near the fault			Fault radius		
		KOBE	LANDERS	BORREGO	NCALIF	SCALIF	
Basic cutting		-34%	-50%	8%	-14%	-15%	-14%
Lateral movement of floors	10th floor	42%	35%	52%	38%	17%	39%
	9th floor	40%	32%	50%	35%	10%	36%
	8th floor	35%	28%	48%	30%	8%	26%
	7th floor	27%	15%	40%	23%	0%	20%
	6th floor	18%	-2%	35%	18%	0%	7%
	5th floor	20%	-15%	33%	20%	7%	11%
	4th floor	7%	-21%	30%	13%	7%	15%
	3th floor	3%	-22%	31%	11%	4%	12%
	2th floor	-1%	-30%	29%	8%	0%	12%
	1th floor	-10%	-33%	8%	3%	-6%	-2%

According to the above tables, it can be said that with the exception of the LANDERS earthquake record, by applying other earthquake records to the structure, the installation of viscous dampers has increased the base shear of the structure. The relative displacement of the floors has mainly decreased with the installation of viscous dampers. With the exception of the case where the Kobe earthquake record has been applied to the structure. The reduction in responses in records near the fault has greater values than records far from the fault.

3.3 Results of analysis of the 15-story structure (base shear and floor displacement)

According to the modeling, the results of modeling the 10-story structure during earthquakes far from and near the fault were examined in two cases without viscous dampers and with viscous dampers. Their results are given in graphs 12 and 13.

According to the above graph, it can be concluded that the displacement of the floors of the structure generally increases more in higher floors than in lower floors.

It is clear from the above graph that the responses of the 10-story steel structure equipped with viscous dampers are also close to each other and it can be concluded that viscous dampers cause uniformity in the deflection of the structures (Table 9).

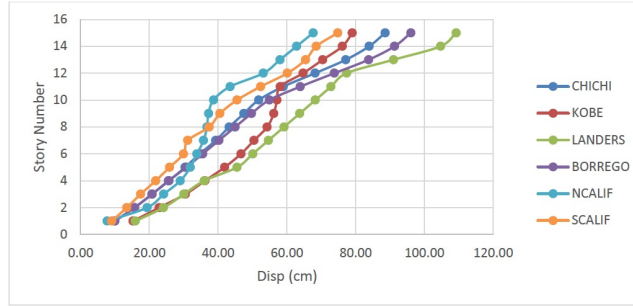


Figure 12: Displacement diagram of a 15-story steel structure without viscous dampers

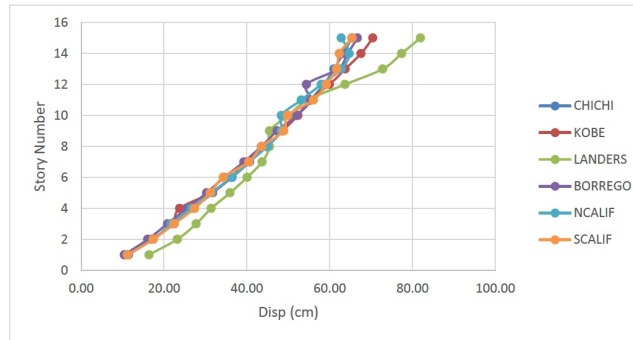


Figure 13: Displacement diagram of a 15-story steel structure equipped with viscous dampers

Table 9: Percentage reduction in structural responses in the state equipped with viscous dampers compared to the state without viscous dampers

	CHICHI	Near the fault				Fault radius	
		KOBE	LANDERS	BORREGO	NCALIF	SCALIF	
Basic cutting	-1%	25%	-5%	-6%	-50%	-20%	
15th floor	26%	11%	25%	31%	7%	13%	
14th floor	25%	11%	26%	30%	-3%	9%	
13th floor	21%	9%	20%	26%	-8%	6%	
12th floor	14%	7%	18%	26%	-9%	2%	
11th floor	6%	5%	25%	13%	-22%	-7%	
10th floor	-1%	8%	27%	5%	-25%	-10%	
9th floor	-2%	14%	29%	5%	-30%	-21%	
Lateral movement of floors							
8th floor	-3%	18%	23%	3%	-22%	-17%	
7th floor	-4%	21%	20%	2%	-14%	-30%	
6th floor	-5%	22%	20%	3%	-7%	-15%	
5th floor	-5%	25%	21%	2%	2%	-20%	
4th floor	-6%	34%	13%	0%	8%	-26%	
3th floor	-9%	28%	8%	0%	10%	-29%	
2th floor	-9%	25%	4%	-3%	10%	-30%	
1th floor	-14%	31%	-3%	-5%	-44%	-24%	

4 Conclusion

This study comprehensively analyzed the seismic effects and dynamic soil-structure interaction on the performance of steel structures. Based on numerical analyses of three structural models with varying heights (5, 10, and 15 stories) on loose soil, the results indicate that both earthquake sequence parameters and soil-structure interaction individually have a significant impact on the dynamic response of a structure. However, when these two factors are considered simultaneously, their combined effects become much more severe, complex, and, in some cases, unpredictable.

A key finding is that the occurrence of consecutive earthquakes, particularly when the initial quake reduces the structure’s effective stiffness, can significantly intensify the dynamic response during the second earthquake. In such a scenario, the system’s natural period changes, increasing the frequency overlap between the structure and the second seismic event. For tall structures where higher modes are strongly excited, this leads to high-amplitude responses, concentrated damage on the upper floors, and entry into the nonlinear behavior region.

Comparing the results, we found that viscous dampers are more effective against near-fault records than far-fault records. The extent to which viscous dampers reduce floor response is not always certain and can even increase depending on the specific earthquake record and structural characteristics. In the 10-story structure, which has a longer fundamental period than the others, the reduction in floor response from using viscous dampers was significantly greater, for both near-fault and far-fault records. The responses of structures equipped with dampers were very similar to each other, and in some cases, almost identical graphically, when compared to the undamped structures.

- Soil-Structure Interaction and Structural Height

The study of dynamic soil-structure interaction also produced noticeable changes. Specifically, for Type II soil (corresponding to Type III in the code), which is deeper and has lower stiffness, the system's natural period increased. This, along with increased foundation movements, higher mode excitation, and greater energy transfer to the structure, led to larger displacements, stress concentrations, and expanded damage zones within structural elements. The accumulation of residual stresses from the first earthquake caused the soil to exit its elastic state and enter the nonlinear region, ultimately intensifying the response in the second quake. Another key finding was the different behavior of short and tall structures. Short-rise structures remained within the linear range, with the interaction having a limited effect. In contrast, tall structures experienced severe displacements, changes in vibration modes, and damage concentrated in the middle and upper floors. These results are consistent with findings from previous shaking table tests and studies, confirming the crucial role of structural height and mode distribution in damage occurrence. In conclusion, ignoring earthquake sequence phenomena and soil-structure interaction in seismic design can lead to inaccurate estimates of a structure's actual response, compromising analytical accuracy. This could have irreparable consequences, particularly for critical projects like bridges, power plants, and high-rise buildings, which are more vulnerable.

- Recommendations and Future Research

It is therefore suggested that advanced nonlinear analyses, which account for earthquake sequences and dynamic interactions as an integral part of the design process, should be used for seismic design, especially in areas with a history of successive earthquakes and sites with deep, soft soils. Furthermore, seismic design codes should explicitly provide guidelines for the numerical modeling of structures that consider earthquake interactions and sequences, enabling a more accurate analysis of structural behavior.

Future research could advance this field by focusing on 3D structural analyses, investigating the effect of more than two earthquake sequences, analyzing the behavior of shallow and deep foundations, considering the simultaneous effect of vertical and lateral loads, and examining the performance of non-steel structures.

References

- [1] B. Aramesh, *Investigation of thermodynamic models and heat transfer during laser radiation in teeth tissue*, J. Popul. Therap. Clinic. Pharmacol. **31** (2024), no. 9, 1362–1377.
- [2] B. Aramesh, A. Enayat, M. Espahbodi, A. Mona Ghannadpour, and S. Honar, *Presenting a new method for reconstructing and revealing metal areas in real raw data (cyanogram improved with tooth filling materials) to reduce the effect of various distortions in two-dimensional scan images of spiral-shaped metal implants and dental P*, Power Syst. Technol. **48** (2024), no. 3.
- [3] O. Araz, *Optimum passive tuned mass damper systems for main structures under harmonic excitation*, Mühendis. Bilim. Tasarım Dergisi **9** (2021), no. 4, 1062–1071.
- [4] O. Araz, *Optimum three-element tuned mass damper for damped main structures under ground acceleration*, El-Cezeri Fen Mühendis. Dergisi **8** (2021), no. 3, 1264–1271.
- [5] M. Badri, S.M. Kazemi, and H. Rahimi, *Presenting the behavioral model of citizens in selection of trip vehicle with emphasis on how to go to work*, Case Stud. Transport Policy **19** (2025), 101304.
- [6] Z. Chang, F. Luca, and K. Goda, *Automated classification of near-fault acceleration pulses using wavelet packets*, Comput.-Aided Civil Infrast. Engin. **34** (2019), no. 7, 569–585.
- [7] Y. Cheng, X. Ji, K. Ikago, and H. Luo, *Analytical solutions of H2 control and efficiencybased design of structural systems equipped with a tuned viscous mass damper*, Struct. Control Health Monitor. **29** (2022), no. 5.
- [8] W. Guo, X.L. Wu, X.N. Wei, Y. Cui, and D. Bu, *Inductance effect of passive electromagnetic dampers on building-damper system subjected to near-fault earthquakes*, Adv. Struct. Eng. **23** (2020), no. 2, 320–333.

- [9] H. He, P. Tan, L. Hao, K. Xu, and Y. Xiang, *Optimal design of tuned viscous mass damper for acceleration response control of civil structures under seismic excitations*, *Engineering Structures*, **252** (2022), p. 113685.
- [10] G. Hu, Y. Wang, W. Huang, B. Li, and B. Luo, *Seismic mitigation performance of structures with viscous dampers under near-fault pulse-type earthquakes*, *Engin. Struct.* **203** (2020), 109878.
- [11] X. Ji, Y. Cheng, and C. Molina Hutt, *Seismic response of a tuned viscous mass damper (TVMD) coupled wall system*, *Engineering Structures*, **225** (2020), 111252.
- [12] X. Kang, Q. Huang, Z. Wu, J. Tang, X. Jiang, and S. Lei, *A review of the tuned mass damper inerter (TMDI) in energy harvesting and vibration control: designs, analysis and applications*, *CMES-Comput. Model. Eng. Sci.* **139** (2024), no. 3, 2361–2398.
- [13] A. Kaveh, M. Fahimi Farzam, and H. Hojat Jalali, *Statistical seismic performance assessment of tuned mass damper inerter*, *Struct. Control Health Monitor.* **27** (2020), no. 10.
- [14] A.E. Kannan and G.H. Powell, *DRAIN-2D: A general purpose computer program for dynamic analysis of inelastic plane structures*, Report No. UCB/ EERC-73/6, Earthquake Engrg. Res. Ctr., Univ. of California, Berkeley, Calif., Apr. 1973.
- [15] S. Khalili Gheidari, *Optimization of process design time in a distributed multi-factory environment using genetic algorithms to organize the process and support the development of technical designs for part production based on information available in the production database*, *Eksplorium-Bul. Pusat Teknol. Bahan Galian Nukli.* **46** (2025), no. 2, 933–954.
- [16] D.P.N. Kontoni and A.A. Farghaly, *The effect of base isolation and tuned mass dampers on the seismic response of RC high-rise buildings considering soil-structure interaction*, *Earthquakes Struct.* **17** (2019), no. 4, 425–434.
- [17] D.P.N. Kontoni and A.A. Farghaly, *TMD effectiveness for steel high-rise building subjected to wind or earthquake including soil-structure interaction*, *Wind Struct.* **30** (2020), no. 4, 423–432.
- [18] S. Li, J. Liu, Z. Yang, X. Bao, F. Wang, X. Wang, and M. Saleh Asheghabadi, *Multiscale method for seismic response of near-source sites*, *Adv. Civil Eng.* **2020** (2020), no. 1, p. 8183272.
- [19] Z. Long, W. Shen, and H. Zhu, *On energy dissipation or harvesting of tuned viscous mass dampers for SDOF structures under seismic excitations*, *Mech. Syst. Signal Process.* **189** (2023), 110087.
- [20] G. Mylonakis and G. Gazetas, *Seismic soil-structure interaction: beneficial or detrimental?*, *J. Earthquake Eng.* **4** (2000), no. 3, 277–301.
- [21] G. Quaranta and F. Mollaioli, *Analysis of near-fault pulse-like seismic signals through variational mode decomposition technique*, *Engin. Struct.* **193** (2019), 121–135.
- [22] T. Salonikios, C. Karakostas, V. Lekidis, and A. Anthonie, *Comparative inelastic pushover analysis of masonry frames*, *J. Struct. Eng.* **25** (2003), 1515–1523.
- [23] S. Shahbazi, I. Mansouri, J.W. Hu, N. Sam Daliri, and A. Karami, *Seismic response of steel SMFs subjected to vertical components of far- and near-field earthquakes with forward directivity effects*, *Adv. Civil Eng.* **2019** (2019), 2647387.
- [24] L. Wang, W. Shi, and Y. Zhou, *Adaptive-passive tuned mass damper for structural aseismic protection including soil-structure interaction*, *Soil Dyn. Earthquake Engin.* **158** (2022), 107298.
- [25] W. Xie and L.M. Sun, *Experimental and numerical investigations on transverse seismic responses of soil-cable-stayed-bridge system subjected to transverse near-fault ground motions*, *Engin. Struct.* **226** (2021), 111361.
- [26] J. Yang, Z. Lu, and P. Li, *Large-scale shaking table test on tall buildings with viscous dampers considering pile-soil-structure interaction*, *Engin. Struct.* **220** (2020), 110960.
- [27] F. Yang, R. Sedaghati, and E. Esmailzadeh, *Vibration suppression of structures using tuned mass damper technology: A state-of-the-art review*, *J. Vib. Control* **28** (2021), no. 7–8, 812–836.